Edge phonoconductivity in a magnetically quantized two-dimensional electron gas

D. J. McKitterick, A. Shik,* A. J. Kent, and M. Henini
Department of Physics, University of Nottingham, University Park, Nottingham NG7 2RD, United Kingdom
(Received 26 July 1993)

Scattering of electrons in edge states of a magnetically quantized two-dimensional electron gas (2DEG) by nonequilibrium acoustic phonons has been studied both experimentally and theoretically. A phonoconductance imaging technique was used to probe the spatial and magnetic-field (B) dependence of the acoustic-phonon scattering of electrons in a GaAs device. It was discovered that a response was observed only when phonons were incident at the edge of the 2DEG. Giant oscillations in the phonoconductance with magnetic field were observed, these were periodic in $1/B$ and changed sign when the field was increased beyond 1.3 T. At low field the oscillations were negative, i.e., phonon scattering causes a decrease in conductance, whereas at high field the oscillations become positive. These results are described theoretically by considering the change in group velocity of the edge electrons upon absorption of a phonon which changes their energy and wave vector. Assuming a sharp edge potential, an important parameter in the theory turns out to be the product of the phonon momentum component parallel to the edge and the magnetic length. If this parameter is greater than unity, then interedge state transitions leading to a decrease in electron group velocity produce the dominant effect, a decrease in conductance. However, if it is less than unity, only intraedge state transitions can take place giving rise to an increase in group velocity and hence an increase in conductance. If the potential at the sample edge is considered to be smooth, which is a more realistic assumption, then the theoretical results remain qualitatively the same, except that the field at which interedge state transitions are no longer possible is reduced in line with the greater separation of the edge channels. This makes it possible to use our results to estimate both the potential gradient at the edge of the sample and the spatial separation of the edge channels. It is also demonstrated that the spatially resolved phonoconductance measurements as a function of magnetic-field strength can be used to probe the local electron concentration and the charge separation connected with the Hall voltage is determined for our sample.

I. INTRODUCTION

The edge state model[1-3] has proved successful in explaining many of the experimental phenomena observed in magnetically quantized two-dimensional electron gases (2DEG's) such as, for example, the integer quantum Hall effect (IQHE). The so-called edge states arise because the electronic wave function must vanish at the physical edges of the 2DEG. This results in the energy of the Landau subbands bending up the sample edges as shown schematically in Fig. 1. Quasi-one-dimensional edge channels are formed where the chemical potential intersects the Landau levels and these carry a proportion of the transport current. The edge channels on opposite sides of a conventional Hall bar carry current in opposite directions and the net edge current is proportional to the difference between the chemical potentials on opposite sides of the sample. Scattering of electrons between edge channels is expected to be weak owing to the small overlap between them (normally the scale of the potential bending at the sample edge is smooth compared to the magnetic length). In this case the resistance of a single 1D channel is given by h/e^2 and the Hall resistance given by h/ne^2, where n is the number of such channels in parallel and which is equal to the Landau-level filling factor. In the edge state model breakdown of the IQHE is attributed to processes which lead to so-called backscattering, which is the transfer of an electron between edge states on opposite sides of the device via an empty or partially filled Landau level.

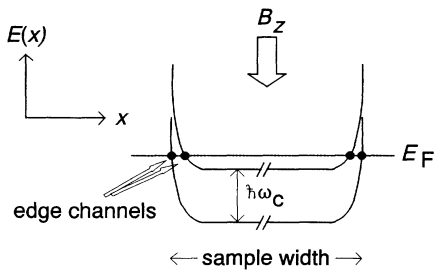

FIG. 1. Variation in Landau-level energy across the width of the device (in this case $\hbar\omega_c \gg eV_H$). The edge channels are formed where the Fermi level intersects the Landau levels.

In order for there to be exact quantization of the Hall resistance in this model it is necessary that there be an equilibrium population of the edge channels on respective sides of the device. However, nonideal current contacts populate different Landau levels to different extents and, if the nonequilibruim distribution reaches another nonideal contact serving as a voltage probe, this can lead to deviation of the Hall resistance from exact quantization and nonzero longitudinal resistance.[3-5] The effects of nonequilibrium edge-state population have been exten-

sively studied using a variety of techniques:[6-9] A strip gate fabricated across the width of a conventional Hall bar can be used to induce backscattering of edge currents.[6,9] Alternatively, point contacts can be used to selectively populate edge channels.[7] It is also possible to create a nonequilibrium distribution of carriers among Landau levels by optical absorption.[8] Some of these results as well as experiments in the nonlocal geometry[10] and on nonlinear resistance scaling[11] indicate that the equilibration lengths for edge channels can be surprisingly large, in excess of 100 μm, in high-mobility devices. All of this means that nonideal contacts can give rise to deviations from exact quantization even in normal-sized devices.

In very pure samples, an important process in establishing equilibrium among edge states is believed to be acoustical-phonon scattering. Acoustic phonons couple to the 2DEG in GaAs via the deformation potential and the piezoelectric effect and, furthermore, the values of energy and wave vector of acoustic phonons compare favorably to the Landau-level separation and magnetic length, respectively, in magnetically quantized 2DEG's. Experimental information regarding phonon scattering of carriers in low-dimensional structures can be obtained more directly by using phonon spectroscopy than it can be obtained by using transport measurements or any other technique. Previously, phonon studies of such systems[12,13] have been limited to looking at bulk effects. More recently, however, a spatially resolving variant of these techniques has been applied to GaAs 2DEG's in the integer quantum Hall regime.[14] In those experiments a pulse of nonequilibrium ballistic phonons was used to stimulate inter-Landau-level transitions which led to a change in the observed two-terminal conductance, the so-called "phonoconductivity" effect. Two-dimensional images of the phonoconductance showed that the transitions preferentially took place at the edges of the device and the effects were attributed to interedge-state tunneling leading to backscattering of electrons.

In this paper we extend our previous work by presenting the results of a more detailed experimental investigation of the phonon scattering of edge states. We also present a detailed theoretical description of the process.

II. EXPERIMENTAL DETAILS

The basic experimental arrangement is shown in Fig. 2. The sample was based on a molecular-beam-epitaxy-grown GaAs/(AlGa)As heterojunction having an electron areal density of about 7×10^{15} m^{-2} and a 4.2-K mobility of ~70 m^{2}V^{-1}s^{-1}. Two device geometries were used; both had active areas of 3 mm (long)$\times$1 mm (wide), one had a single pair of Au-Ge contacts at the ends while the other, a conventional Hall bar, had additional paris of potential probe contacts separated by 2 mm along each side of the device. The back face of the 380-μm-thick semi-insulating (Cr-free) (001) GaAs substrate was polished and a 100-nm-thick layer of Cu-Ni deposited by vacuum evaporation. The sample was mounted in a optical-access helium cryomagnetic system providing a maximum field of 7 T and minimum temperature of about 1.5 K.

Nonequilibrium phonons were generated by absorbing the radiation from a pulsed (pulse length$\approx$100 ns) Nd-YAG (yttrium aluminum garnet) laser in the Cu-Ni film. The spectrum of generated phonons was approximately Planckian with a peak at $\omega_{\max}=3k_BT_h/\hbar$, where T_h is the temperature of the laser-heated spot. Knowing the laser power P_1 absorbed in the film it was possible to determine T_h by applying acoustic mismatch theory:[15]

$$\frac{P_1}{A}=524(T_h^4-T_0^4)\ .$$

Here T_0 is the substrate background temperature and A is the area of the focused laser spot, about 2.5×10^{-9} m^2. In our case T_h was about 10 K giving $\omega_{\max}/2\pi\approx600$ GHz. The phonon pulse traveled ballistically across the substrate which was at about 2 K and fell upon the 2DEG. The electron-phonon interaction caused a small transient change in the device resistance which was observed by passing a constant current and measuring the change in the potential drop along the device. The signal, which typically amounted to a few microvolts, was fed via a high-impedance preamplifier to a boxcar integrator. An example of the signal after averaging is shown in Fig. 3; normally we are only interested in the in-

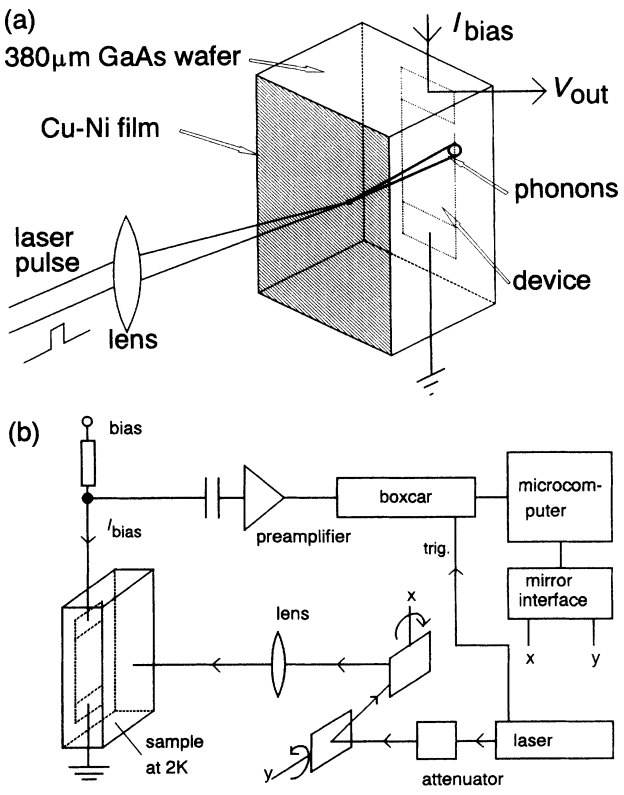

FIG. 2. (a) Sample geometry: nonequilibrium phonons are generated by thermalizing a pulsed laser in a Cu-Ni film. These propagate across the GaAs substrate ballistically and interact with the 2DEG giving rise to a transient change in V_{out} at constant bias current. (b) Schematic diagram of the full imaging system: The laser beam is positioned using a pair of galvanometer-driven mirrors and the signal is recorded as a function of the beam position.

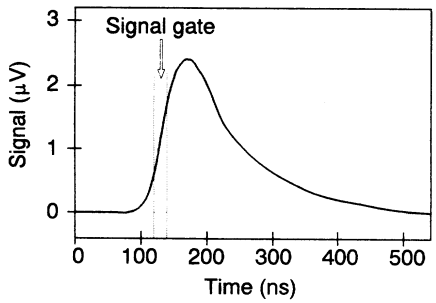

FIG. 3. Signal following the laser pulse at $t=0$, the boxcar gate is set to select the part of the signal due to those phonons that have traveled the most direct path across the substrate.

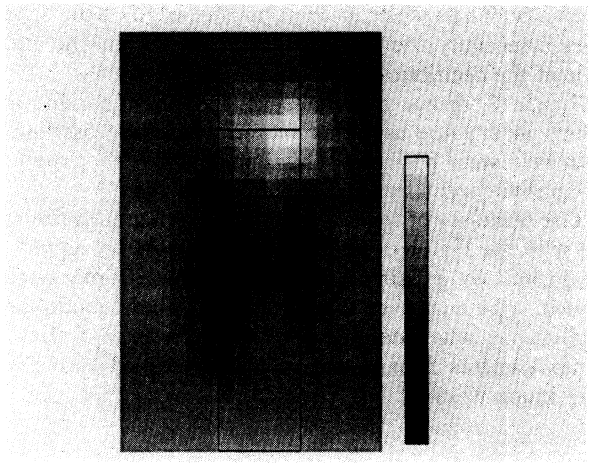

FIG. 4. 2D image of the sample response at integer filling factor (magnetic field 1.5 T, directed into paper; current 50 μA, up). The dark regions at the edges of the sample are due to a decrease in conductance when the phonons are incident there. Note also the activated behavior (bright region) when the phonons are incident at the point where current exits (electrons enter) the 2DEG.

tensity of the signal which is sampled by the boxcar gate at a fixed delay as indicated in the diagram.

Owing to the phenomenon of phonon focusing,[16] the flux of transverse-acoustic (TA) modes traveling close to the [001] direction, i.e., near normal to the 2DEG, is considerably larger than in other directions. The area of this much-enhanced phonon flux subtends an angle of about 12° at the point of generation. This means that the detected signal corresponded largely to the interaction of TA phonons with an area of the 2DEG about 100 μm across directly opposite the phonon source. Longitudinal-acoustic (LA) modes are not focused significantly, however, the time of flight, which is proportional to the distance traveled by the phonons, depends on the angle of propagation relative to the [001]. By using a narrow boxcar gate ($\approx$20 ns) starting at the time taken by the phonons to traverse the substrate along the [001] direction (about 70 ns), we could ensure that the signal corresponds to the interaction of LA modes with an area of the 2DEG about 100 μm across. Therefore, for whatever mode we chose to look at, the area being probed is sufficiently small to discriminate between edge and bulk effects when using a 1-mm-wide 2DEG.

By using a pair of computer-controlled galvanometer mirrors to raster scan the laser spot an image of the phonoconductance effects could be built up. Alternatively, the laser spot might be fixed at one position, say, opposite an edge, and the phonoconductance recorded as a function of magnetic-field strength.

III. RESULTS

Figure 4 shows an image of the TA-mode phonoconductance of the two-terminal device, taken at a field of 1.5 T which corresponds to a Landau-level filling factor of 10. It is clear from the image that in this case the only response from the active part of the device is a transient decrease in conductance when the phonons are incident at the sample edges. In most cases the two edges did not respond equally, the relative response being very sensitive to the filling factor. If an unequal response was observed it was found to swap sides upon magnetic-field or current reversal.[14] Also noticeable in the image is a transient decrease in conductance when the phonons are incident at the current exit contact. Regardless of current or magnetic-field direction the contact response is always strongest near the point where the electrons enter the 2DEG from the contact. We attribute this response to thermal activation of carriers in the disordered contact region, these may be injected into the 2DEG causing an increase in the two terminal conductance. This effect has also been observed in silicon metal-oxide-semiconductor-field-effect transistor devices.[17]

Figure 5 shows the variation of the TA phonoconductance of the two-terminal device with magnetic field. The point of phonon generation was opposite the edge of the device and half-way along its length, well away from the contacts, as shown in the inset. There are a number of points which we will note here without discussion; a detailed discussion will follow in Sec. V, after the theory. (i) The most striking feature is that giant oscillations are observed even at very low magnetic-field strengths where the Shubnikov–de Haas oscillations are almost impossible to discern. (ii) Although the oscillations are large, the absolute amplitude of them is tiny compared to the average dc conductance G. The largest changes in device conductance, ΔG, owing to phonon absorption were at the most a mere $10^{-4}\%$ of the total conductance at the same magnetic-field strength. (iii) At low magnetic-field strength the oscillations are negative (i.e., increasing resistance) and they are nearly in phase with the Shubnikov–de Haas oscillations, while above 1.5 T the oscillations become positive. (iv) At high magnetic fields and at values of filling factor corresponding to the Fermi level being mid-spin-split gap a negative peak (with respect to the background) in the phonoconductance is seen. The size of this peak increases rapidly with decreasing filling factor. It is clear from the image in Fig. 6 that the signal associated with spin-split levels is a bulk

effect. (v) The results at the opposite edge of the sample were essentially the same, Fig. 7, except that the amplitude of the oscillations is smaller.

Figure 8 shows an image of the phonoconductance effects at a value of filling factor where the oscillations with field were positive. This image shows that the positive phonoconductivity is also an edge effect.

The same set of measurements were made on the sample with the Hall bar geometry; in this case the signal was monitored on a pair of potential probes on one edge of device. The nature of the images and phonoconductivity oscillations was qualitatively the same except that the contact effects seen in Fig. 4 and described above were very much weaker.

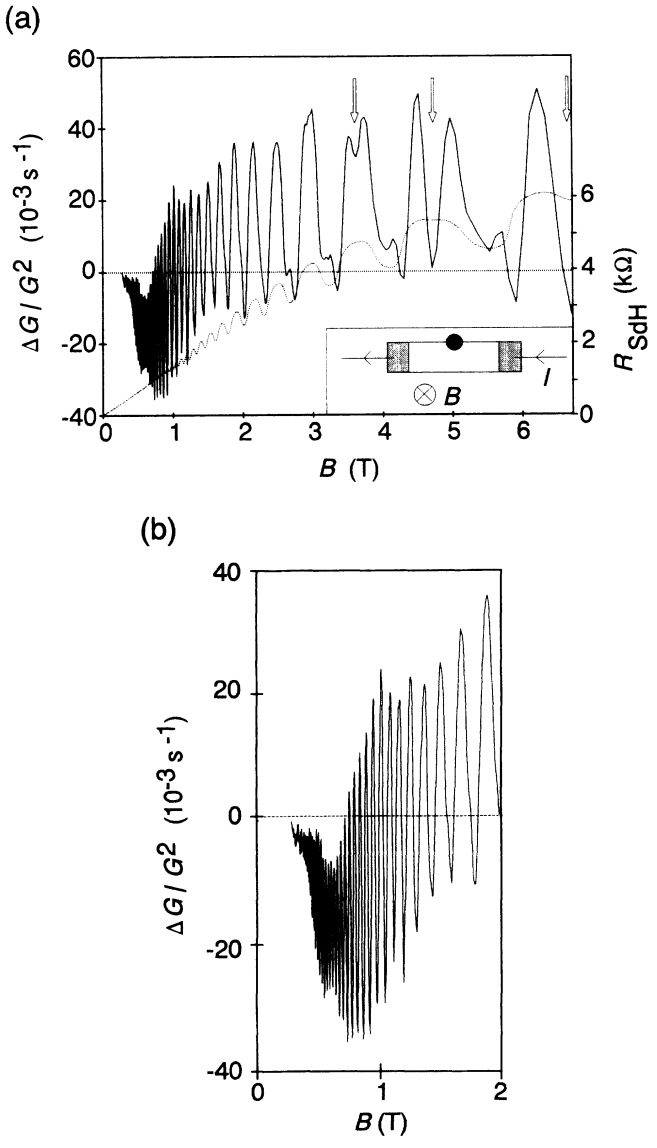

FIG. 5. (a) Magnetic-field dependence of the edge phonoconductivity. The edge being probed and the magnetic field and current directions are shown in the inset, the positions of the spin-split peaks are indicated by the arrows. Also shown (dotted line) for comparison are the two-terminal Shubnikov–de Haas oscillations. (b) Closeup of the region below 2 T.

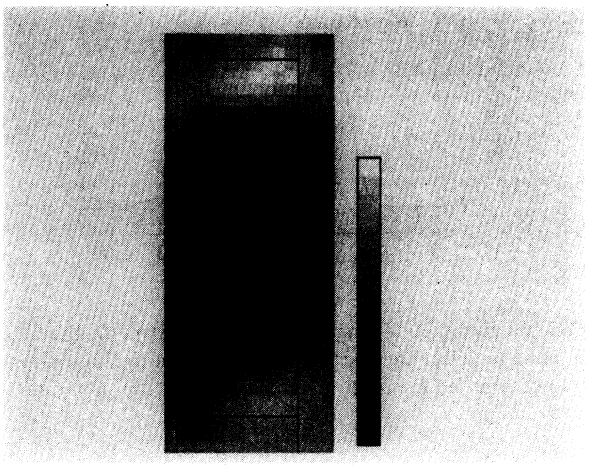

FIG. 6. Image of the phonoconductivity response on one of the spin-split peaks (field and current directions as in Fig. 4).

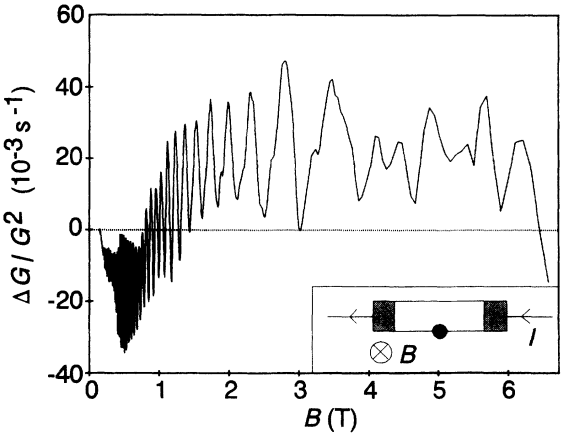

FIG. 7. Variation with magnetic field of the phonoconductivity at the opposite edge to that in Fig. 5.

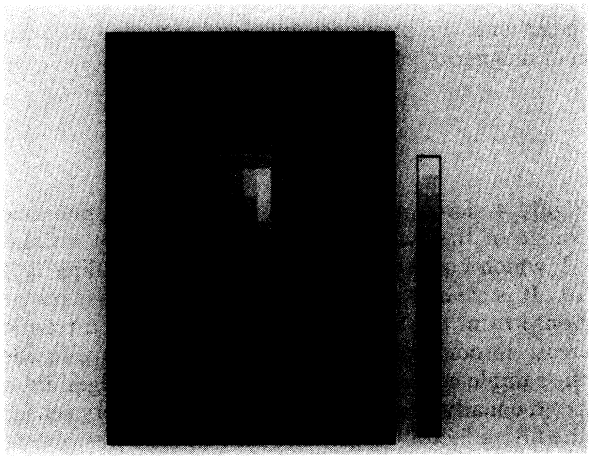

FIG. 8. Image of the positive phonoconductivity showing that this too is an edge effect.

IV. THEORY

A. General expressions

We will now consider theoretically the influence of nonequilibrium phonons with wave vector **q** on the 2DEG conductivity in a quantizing magnetic field $\mathbf{B}\|z$. If the phonon frequency $\omega=sq$ (s is the sound velocity) is less than the cyclotron frequency ω_c, the phonons cannot cause inter-Landau-level transitions in the bulk of the sample. The absorption is possible only near the sample edges where the energy of levels depends on the position of the Landau oscillator center X_0, or on the wave vector k parallel to the edge and proportional to X_0: $k=X_0/l_B^2$ where $l_B=(\hbar/eB)^{1/2}$ (see Fig. 9).

Initially we shall assume that the sample edge at $X=0$ is a sharp, infinitely high wall, then energies $\epsilon_N(k)$ and wave functions $|N,\epsilon\rangle$ are determined by the Schrödinger equation with a parabolic potential and zero boundary condition at $X=0$.

The phonoconductivity (PC) is caused by the fact that the electrons absorbing the phonons change their wave vector k, their group velocity $v_N(\epsilon)=\hbar^{-1}\partial\epsilon_N/\partial k$ and, hence, their contribution to the edge current j. Formally, PC can be expressed in terms of electron distribution functions at different levels $f_N(\epsilon)$. If $\Delta f_N(\epsilon)=f_N(\epsilon)-f_0(\epsilon)$ (f_0 is the Fermi function) then

$$\Delta j=e\sum_N\int v_N(\epsilon)g_N(\epsilon)\Delta f_N(\epsilon)d\epsilon=\frac{e}{2\pi\hbar}\sum_N\int\Delta f_N(\epsilon)d\epsilon\ . \tag{1}$$

Here $g_N(\epsilon)=[2\pi\hbar v_N(\epsilon)]^{-1}$ is the one-dimensional density of states.[3]

In a degenerate electron system the nonequilibrium part of the distribution function can be written in the following form:

$$\Delta f_N(\epsilon)=\tau_N(\epsilon)\sum_M\left[\int_{E_F-\hbar sq}^{E_F}g_M(\epsilon')W_{M\epsilon'}^{N\epsilon}(\mathbf{q})d\epsilon'-\int_{E_F}^{E_F+\hbar sq}g_M(\epsilon')W_{N\epsilon}^{M\epsilon'}(\mathbf{q})d\epsilon'\right]. \tag{2}$$

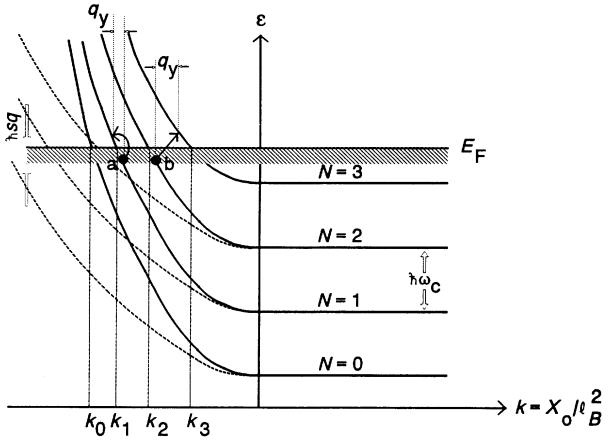

FIG. 9. Dependence of the Landau-level energies on the position of the cyclotron orbit center for a sharp edge (solid lines) and smooth edge (dotted lines) potential. The position of the Fermi level is shown and the shaded area indicates the range of energies in which electrons can absorb phonons. The two types of transitions, intralevel (a) and interlevel (b), are shown.

Here τ_N is the relaxation time, E_F is the Fermi energy, and $W_{N\epsilon}^{M\epsilon'}(q)$ is the probability of transition $|N,\epsilon\rangle\rightarrow|M,\epsilon'\rangle$ caused by phonons with the wave vector **q**.

We shall describe the electron-phonon interaction by the usual potential $V=\Lambda q^\gamma/\Omega^{1/2}\exp(i\mathbf{q}\cdot\mathbf{r})$ (Ω is the normalizing volume, γ is equal to 1 for deformation and to -1 for piezoelectric-phonon potential, and Λ is a constant.) Let us consider electron transitions between states $|N,\epsilon\rangle$ and $|M,\epsilon'\rangle$ caused by this potential. For edge-state electrons the y component of momentum is conserved: $k'=k+q_y$ so the transition probability

$$W_{N\epsilon}^{M\epsilon'}(q)=\frac{2\pi\Lambda}{\hbar\Omega}q^\gamma|\langle N,\epsilon|\exp(i\mathbf{q}\cdot\mathbf{r})|M,\epsilon'\rangle|^2\times\delta[\epsilon_N(k)-\epsilon'_M(k+q_y)+\hbar sq]\ . \tag{3}$$

If the values of ϵ and ϵ' determined by the δ function in (3) lie inside the corresponding integration limits in (1) and (2), then the expression for the current can be transformed to the form

$$\Delta j=\frac{e\Lambda}{2\pi S\hbar^3}q^\gamma\sum_{M,N}\int_{E_F}^{E_F+\hbar sq}|\langle N,\epsilon|\exp(i\mathbf{q}\cdot\mathbf{r})|M,\epsilon-\hbar sq\rangle|^2\left[\frac{\tau_N(\epsilon)}{v_M(\epsilon-\hbar sq)}-\frac{\tau_M(\epsilon-\hbar sq)}{v_N(\epsilon)}\right]d\epsilon\ , \tag{4}$$

where S is the sample area.

So, we see that PC is determined by three factors: (i) the electron-phonon matrix element; (ii) the difference of electron velocities in the initial and final states; (iii) the difference of relaxation times for the excitations above and beneath the Fermi level.

The dependencies of the PC on the phonon wave vector **q** and on the magnetic field B which we are interested in, are governed by all three factors. Let us study them in series.

The dependence of the matrix element on q_x and q_y is determined by the properties of wave functions $|N,\epsilon\rangle$ and so far has been analyzed only for the limiting cases $k\rightarrow-\infty$ (triangular well) (Ref. 18) and $k\rightarrow\infty$ (far from the edge).[19] The basic qualitative properties of these elements can, however, be deduced. If the sample edge is sharp, there is only one characteristic length in the Schrödinger equation, namely, l_B. Therefore, the matrix elements become negligibly small at $|q_x|,|q_y|\gg l_B^{-1}$. The behavior of $\langle N,\epsilon|\exp(i\mathbf{q}\cdot\mathbf{r})|M,\epsilon'\rangle$ at small q_x and q_y is

determined by orthogonality of the wave functions: the diagonal ($N=M$) elements tend to unity and nondiagonal ($N\neq M$) elements tend to zero. The latter fact means that the nondiagonal elements being considered as functions of q_x or q_y have a maximum at $|q_x l_B|\sim 1$ or $|q_y l_B|\sim 1$.

We assume that the phonon wave-vector component q_z normal to the plane of original 2DEG is less than π/a where a is the confinement length for the 2DEG. In this case the matrix elements of $\exp(i\mathbf{q}\cdot\mathbf{r})$ do not depend on q_z. More accurate calculations using the wave functions for a triangular quantum well near the heterointerface show that for GaAs this assumption is valid for $q_z\sim 1.4\times 10^8(N_s/10^{15}\ \mathrm{m}^{-2})^{1/3}\ \mathrm{m}^{-1}$, where N_s is the 2DEG areal density. If $N_s\approx 7\times 10^{15}\ \mathrm{m}^{-2}$ it corresponds to phonon frequencies of about 200 GHz.

The second factor, $\nu_N(\epsilon)-\nu_M(\epsilon')$, is considerably different for intralevel ($N=M$) and interlevel ($N\neq M$) transitions. If $kT_0,\hbar sq\ll\hbar\omega_c$, then all electron transitions take place in the vicinity of the Fermi energy E_F and we can expand the dispersion law $\epsilon_N(k)$ near E_F. It is convenient to introduce the following notations:

$$\nu_N\equiv\nu_N(E_F)=-\hbar^{-1}\left.\frac{\partial\epsilon_N}{\partial k}\right|_{\epsilon=E_F},$$

$$m_N^{-1}=\hbar^{-2}\left.\frac{\partial^2\epsilon_N}{\partial k^2}\right|_{\epsilon=E_F}.$$

Then

$$\nu_N(\epsilon)-\nu_N(\epsilon')\simeq\frac{\hbar q_y}{m_N}=\frac{\hbar sq}{m_n\nu_N}, \tag{5}$$

whereas for $N\neq M$, $\nu_N(\epsilon)-\nu_M(\epsilon')\simeq\nu_N-\nu_M$.

The expression for the relaxation time τ depends on the relaxation mechanisms. Two of them are the most importance: the acoustic-phonon emission and interlevel impurity scattering. Other scattering mechanisms in one-dimensional edge states are suppressed to some extent. Intralevel elastic impurity scattering is absent in the conditions of quantum Hall effect.[3] Intralevel electron-electron scattering vanishes since the momentum and energy conservation laws allow only processes when indistinguishable particles simply exchange momentum and energy during binary collisions.[20,21] Interlevel electron-electron scattering may take place but it is connected with the large energy exchange ($\sim\hbar\omega_c$) and, therefore, is absent in the case when both the phonon energy $\hbar sq$ and the thermal spreading of the Fermi distribution kT_0 are much less than $\hbar\omega_c$.

Theoretical expressions for interlevel relaxation time determined by both phonon and impurity scattering can be found in Refs. 9 and 22. For intralevel phonon scattering these can be obtained directly from (3). We shall not discuss the exact formulas for τ but note that in any case the scattering probability is proportional to the density of states and hence,

$$\tau_N(\epsilon)\sim\nu_N\ . \tag{6}$$

Taking into account the inequality $\hbar sq\ll\hbar\omega_c$, E_F, and using (6) we can eventually rewrite (4):

$$\Delta j=\sum_{M,N}A_{MN}|\langle N,E_F|\exp(i\mathbf{q}\cdot\mathbf{r})|M,E_F\rangle|^2\times\left[\frac{\nu_N^2(E_F)-\nu_M^2(E_F-\hbar sq)}{\nu_M\nu_N}\right]. \tag{7}$$

Now we shall apply the expression (7) for determination of some of the characteristics of PC. An important role in the theory is played by the dimensionless parameter ql_B. If phonons are generated by a local heat source with the temperature T_h, this parameter for n-type GaAs can be estimated at $0.66T_h/\sqrt{B}$. One can see that it may be larger and smaller than unity. We shall consider both situations assuming for simplicity the sample temperature to be zero. In practice it means that kT_0 must be much less than the energy of nonequilibrium phonons $\hbar sq$.

B. High magnetic fields ($ql_B\ll 1$)

At $ql_B\ll 1$ the matrix element in (7) is equal to δ_{MN} which means that only intralevel (intrasubband) transitions can be induced by the phonons under consideration. First of all note that inside any subband the electron velocity ν increases with the energy. This means that the phonon absorption causes the increase of current and, hence, PC is always positive.

For intralevel transitions all diagonal coefficients A_{NN} are of the same order, and after substitution of (5) and (7), we obtain

$$\Delta j\sim\sum_N\frac{1}{m_N\nu_N^2}\ . \tag{8}$$

Let us remember that the PC has nonzero value given by (8) only if the initial electron energy $\epsilon(k_0)$ determined by the equation $\epsilon(k_0+q_y)+\hbar sq$ lies in the interval $E_F-\hbar sq<\epsilon(k_0)<E_F$. This restricts possible wave vectors of phonons causing PC. The analysis shows that phonons are "active" (that is, they may interact with the edge-state electrons) if the directions of their momenta lie in narrow but finite angular interval $\Delta\phi\approx\hbar s^2q/m_N\nu_N^3$ near $\phi=\cos^{-1}(s/\nu_N)$. For the most subbands except, maybe, the highest, $\nu_N\sim l_B\omega_c$. The latter quantity is, as a rule, much more than s. For instance, in n-type GaAs at $B=2$ T, $s/l_B\omega_c\simeq 8\times 10^{-2}$. This means that the edge-state electrons can interact only with the phonons with $\phi\simeq\pi/2$, that is propagating almost normally to the sample edge. This fact has already been pointed out in Refs. 18, 23, and 24.

The field dependence of PC is determined by that of the quantities ν_N and m_N in (8). The increase of B shifts up all dispersion curves in Fig. 9 (the scale of the abscissa also changes) which results in the decrease of ν_N and increase of m_N. For E_F approaching any particular Landau level from above, $m_N\to\infty$, $\nu_N\to 0$. The product $m_N\nu_N^2$ in this limit tends to zero which can be shown with the help of analytical expressions for $\epsilon_N(k)$ in the limit $k\to\infty$ obtained in Ref. 25. This means that as $E_F\to\hbar\omega_c(N+\frac{1}{2})$, PC increases which can be explained, at least partially, as resulting from the singularities in the one-dimensional density of states. The growth of PC is, however, limited: In the closest vicinity of $\hbar\omega(N+\frac{1}{2})$, ν_N

becomes less than s, phonon absorption becomes impossible, and the contribution of the corresponding Landau level drops to zero very sharply, in a small energy interval $\Delta E_F = \hbar s q$.

It can be also seen that the increase of ϕ at E_F approaching some Landau level in the bulk is accompanied by the growing of $\Delta\phi$. This means that PC may be caused by phonons propagating in wider direction range (which is one more reason for PC to increase). It is connected with the decrease of the Fermi velocities v_N widening the corresponding Čerenkov cones, especially for the highest subband.

The resulting dependence of PC on the Fermi-level position caused by all Landau levels is shown in Fig. 10. One can clearly see the giant oscillations in it.

C. Low magnetic fields ($ql_B \gg 1$)

At $ql_B \gg 1$ both intralevel and interlevel transitions are possible. Hence PC will contain two terms which will be named Δj_1 and Δj_2. The expression for Δj_1 has much in common with the case $ql_B \ll 1$ considered above and Eq. (8) is still valid but in the more restricted range of E_F. If $E_F \to \hbar\omega_c(N+\frac{1}{2})$ and $v_N \to 0$, then PC after its initial increase, described by (8), begins to drop drastically not at $v_N \simeq s$, but earlier, at $v_N \simeq sql_B$. According to the energy conservation law, $q_y \simeq qs/v_N$, and therefore, at $v_N < sql_B$, q_y exceeds l_B^{-1} resulting in the decrease of the matrix element and, hence, of PC. As a result, the oscillations of Δj_1 with E_F will have smaller amplitude than in the case $ql_B \ll 1$ (see Fig. 10).

For the interlevel PC component Δj_2, we may neglect the phonon energy $\hbar sq$ in the argument of v_M. As a result, the numerator in (7) becomes equal to $v_N - v_M$ which can be both positive (for transitions to lower level) and negative (for transitions to higher level). For a fixed value of q_y, the sum in (7) contains only one (or no one) term. The angular distribution of "active" phonons consists of very narrow intervals: $\Delta\phi \simeq s|v_N - v_M|/v_N v_M$ near the values $\phi = \cos^{-1}[(k_M - k_N)/q]$. Note that positive PC is caused by phonons with positive values of q_y and vice versa.

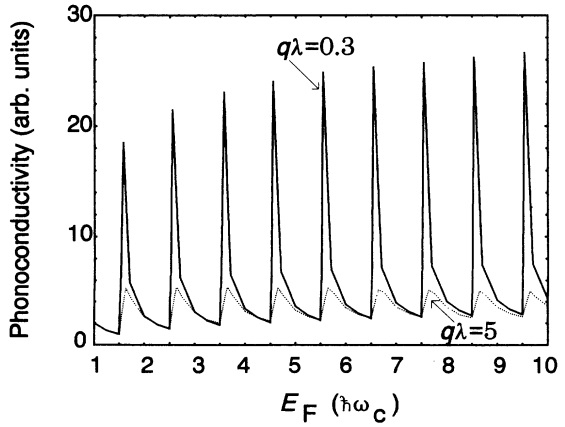

FIG. 10. Dependence of the intralevel PC on the Fermi level position for $ql_B = 0.3$ and $ql_B = 5$.

For large phonon frequency sq all active angles ϕ are close to the normal to the 2DEG (z axis). If the phonon momentum components q_y in a real experiment are distributed in a relatively wide interval around the z axis, then all nondiagonal coefficients A_{MN} in (7) are of the same order. In this case Δj_2 is always negative. This fact can be easily explained as follows: The main contribution to the sum is made by the transitions to the level closest to the Fermi energy and having maximal density of states. But the transitions to this level are possible only from the lower levels with larger v_N which results in a negative PC.

Equation (7), as well as our previous expressions, is in some sense oversimplified. In fact, as $E_F \to \hbar\omega_c(M+\frac{1}{2})$, when $k_M \to \infty$ and $v_M \to 0$, (7) does not tend to infinity but drops sharply after reaching some maximal value. A similar effect has already been discussed for intralevel transitions. It results from the fact that the wave functions of the state with large k_M, and, hence, large X_0, and of other edge states overlap only slightly and the corresponding electron-phonon matrix element is very small. As a result, the PC vs E_F dependence will remind us of that for intralevel transitions (curve 2 in Fig. 10) but the PC itself will be negative.

The total PC of the sample at low field is given by the sum of intralevel and interlevel processes. Their relative intensity is determined by the ratio of diagonal and nondiagonal coefficients A_{MN} which are, in turn, proportional to the corresponding relaxation times. For intralevel processes relaxation is due to acoustic-phonon emission. For interlevel processes, however, this emission is in many cases impossible. As one can see from Fig. 9, the component q_y for phonons emitted in interlevel processes is approximately equal to $k_N - k_M$. Hence, their energy always exceeds $\hbar s|k_N - k_M|$. This means that nonequilibrium electrons excited to the states with the energy $\epsilon < E_F - \hbar s|k_N - k_M|$ cannot emit an interlevel phonon since at $T_0 = 0$ there are no unoccupied states below E_F. The excess momentum $k_N - k_M$ can be given away only in the processes of impurity scattering discussed in Refs. 20 and 22. This means that, at least for high-mobility samples, τ for interlevel processes exceeds that for intralevel ones. Since at the same time the phonon-induced change of the electron velocity $v_N - v_M$ for interlevel processes is considerably more, the resulting PC is expected to be negative.

Comparing this conclusion with the result of the previous section, we see that at magnetic fields satisfying the condition $qlB \simeq 1$, PC must change its sign.

D. Smooth-edge potential

So far in our calculations we have considered the sample edge to be an infinitely sharp potential well. However, in reality a smooth edge potential is believed to be more realistic.[9,26] The smooth character of the edge does not change the main qualitative conclusions but it does inhibit the electron-phonon processes near the edge and, hence, modifies some of the quantitative estimates. On the one hand, the condition for interlevel processes to occur becomes more severe than $ql_B > 1$ since the states

at the Fermi surface belonging to different levels are separated by a larger distance ΔX_0 and, therefore, require larger momentum transfer $k_N - k_M$ (dashed curves in Fig. 9). The amplitude of PC will diminish in smooth-edge structures much less than the phonon absorption since for the same reasons the relaxation time will also increase.[3] On the other hand, intraband processes are also more restricted. From Fig. 9 one sees that for the smooth edge the group velocity v_N is less and the condition $s > v_N$ under which electron-phonon processes vanish, is fulfilled in a wider interval of parameters. At the same time this leads to a decrease of the allowed angle between the sample edge and the phonon momentum.

One of the models of the smooth edge, namely, that of a parabolic confining potential $m\omega_0^2 X^2/2$, was used in Ref. 9 for calculating the interlevel scattering processes. This model can be applied to the PC theory as well. In this model the interlevel transitions will be caused only by phonons with $q_y > (m\omega/\hbar)^{1/2}\omega/\omega_0 = l_B^{-1}\omega^{3/2}\omega_0^{-1}\omega_c^{-1/2} \gg l_B^{-1}$, where $\omega = (\omega_0^2 - \omega_c^2)^{1/2}$. As for the intralevel PC, it can be calculated by (5) where we must assume $m_N = m\omega^2/\omega_0^2$ and $v_N = \{2m[E_F/\hbar - \omega(N+\frac{1}{2})]\}^{1/2}\omega_0/\omega$. The result is shown in Fig. 11 for two different values of ω_0. The smoothing of the edge (decrease of ω_0) is seen to reduce the PC oscillations notably.

If the sample edge is approximated by a linear rather than parabolic potential, the main results are physically more transparent. The spatial separation of the edge channels is $\hbar\omega_c/\nabla V$, where ∇V is the potential gradient at the edge. Therefore, interlevel transitions can only be caused by phonons with

$$q_y \geq \frac{\hbar\omega_c}{\nabla V l_B^2} . \tag{9}$$

The edge phonoconductivity vanishes altogether if the potential gradient at the edge is less than seB owing to the fact that the Hall drift velocity $\nabla V/eB$ becomes less than the sound velocity which prevents phonon absorption. This is presumably the case for metal-oxide-semiconductor silicon devices with large oxide thickness in which no edge phonoconductivity was observed experimentally.[17]

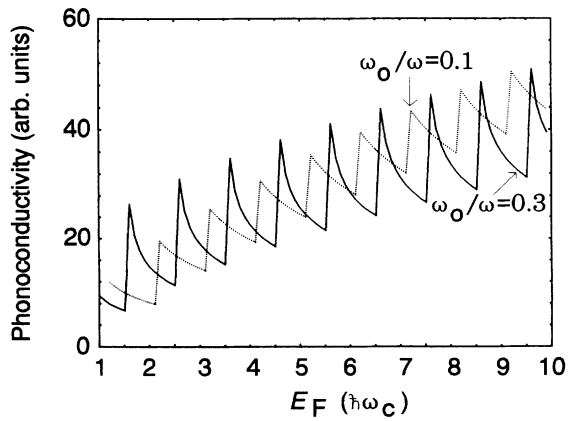

FIG. 11. Dependence of the intralevel PC on the Fermi level position for a structure with parabolic confinement with $\omega_0/\omega = 0.3$ and $\omega_0/\omega = 0.1$.

V. DISCUSSION

We are now in a position to discuss the experimental results in Sec. III in light of the theory in Sec. IV. First, we note that the observed effect is connected with electron transitions near the edges rather than in the bulk of the sample. This is in line with theoretical estimates: In the experimental conditions the phonons which produce observable effects are those which propagate close to the normal to the 2DEG which means that $q \approx q_z$. According to the estimates in the previous section, the form factor caused by the finite width of the potential well in the z direction supresses the electron-phonon interaction for phonon frequencies exceeding 200 GHz. The Landau-level separation in the bulk exceeds this value at all fields above 0.5 T and so phonons which may cause interlevel transitions in the bulk interact with the 2DEG very weakly. This is not so in the case of the spin-split levels, where the splitting is much smaller, typically a few tens of GHz (Ref. 27) and consequently bulk transitions are possible (Fig. 6).

In agreement with the theoretical predictions, the field dependence of the PC has the oscillating character. The oscillation frequency is close to that of the Shubnikov–de Haas (SdH) effect, but the shape of the oscillations is considerably different. For most values of B the SdH oscillations have relatively small amplitude on a monotonically increasing background. The PC exhibits giant oscillations with $\Delta G_{\max}/\Delta G_{\min} \gg 1$ even in a relatively low field, $B \sim 1$ T, in good agreement with the theoretical results shown in Fig. 10.

The most remarkable feature is the change of sign of the PC at $B_c \approx 1.2$ T. In lower fields the PC oscillates, remaining always negative, while in higher fields both maxima and minima of PC have positive sign. The theoretical description of this is contained in Sec. IV. At high magnetic field the energy and momentum separation between the different edge channels is too large and phonons with a given q can only cause intralevel transitions giving rise to positive PC. At $B < B_c$ interlevel processes become dominant and PC acquires negative sign. It should be pointed out that the amplitude of the positive PC is actually very much smaller than that of the negative PC; they appear the same in the figure because of the effect of the background monotonic change in G which reduces rapidly with increasing B.

It is interesting to compare the numerical value of B_c with the theory. According to the results of Sec. IV, in the case of a sharp edge, the critical magnetic field is to be determined from the condition $q_y l_B \approx 1$. In our experiments q_y does not have a strictly definite value since the phonons are not monochromatic and their angle of incidence varies along the sample edge. Assuming the peak in the Planckian distribution of phonons to be well above the form-factor imposed cutoff frequency, 200 GHz, then most of the phonons that are able to interact with the 2DEG will be in the region of 200 GHz. The gate selec-

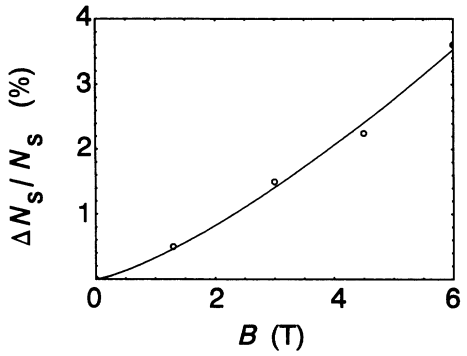

FIG. 12. Variation in ΔN_s with magnetic field. The effects of inhomogeneity have been canceled by making measurements for both current directions.

tion (see Sec. II and Fig. 3) ensures that only phonons incident at up to about 12° to the normal contribute to the PC. Combining these gives an average value of q_y in the region of 10^8 m^{-1}. Using this we obtain $B_c \approx 5$ T which is considerably more than the experimental value. This means that the sample edge is of graded rather than sharp character, in agreement with the results[9,25] obtained also for GaAs/(AlGa)As heterostructures. Substituting the above estimate for q_y and the experimental value for B_c into Eq. (9) we obtain $\nabla V \approx 2\times 10^4$ eV m^{-1}, assuming a linear potential gradient.

The period of oscillation of the PC should be dependent on the electron density at the point being probed. It therefore appears strange that the period of oscillation is nearly the same at both edges of the sample as shown by Figs. 5(a) and 7 since there should be a charge separation $e\Delta N_s$ which is connected with the Hall voltage. However, when the bias current was reversed, a considerable difference in the oscillation periods was observed, amounting to about 6% at 6 T. These results point to inhomogeneity in the electron density across the device, for one direction of current ΔN_s just compensates for the inhomogeneity, while for the opposite current direction the difference in carrier concentration between the edges is enhanced. This conclusion was confirmed by making measurements at other values of bias current and we could deduce that the gradient in the carrier density due to inhomogeneity was 2%, which was independent of the current or magnetic-field strength. Figure 12 shows ΔN_s as a function of the magnetic-field strength at a current of 50 μA after removing the effect of inhomogeneity. It is possible to estimate the difference in electron concentration between the two edges using the formula

$$\Delta N_s = \frac{CV_H}{el_B} ,$$

where C is the capacitance per unit length of the edge states which is expected to be weakly field dependent. For our sample we obtain $\Delta N_s / N_s \approx 4.3\%$ at 4.5 T, which is not out of line with the experimental results in spite of the very approximate nature of the calculation.

VI. CONCLUSIONS

The conductivity of a 2DEG can be altered by a flux of nonequilibrium phonons. This effect, phonoconductivity, has been studied experimentally and theoretically for a magnetically quantized 2DEG. If the bulk Landau-level separation $\hbar\omega_c$ exceeds the phonon energy $\hbar sq$, phonons can cause transitions only near the sample edge. These transitions change the group velocity of the electrons and, therefore, the electric current. The net PC depends nonmonotonously on the position of the Fermi level being maximal when it is close to the energy of any Landau level in the bulk. Giant oscillations are observed. At low magnetic-field strengths $B < 1.2$ T, interedge-state transitions leading to a reduction in the conductivity took place. At larger magnetic-field strengths intra-edge-state transitions dominated giving rise to an increase in conductivity. The field at which changeover occurs is related to the sharpness of the potential gradient at the edge; we obtain a value of approximately 2×10^4 eV m^{-1} which gives a separation of the edge states of about 100 nm T^{-1}. At high fields where spin splitting of the Landau levels is resolved, bulk transitions between the spin-split levels can be induced by nonequilibrium phonons giving rise to a decrease in conductivity.

This spatially resolving technique is also able to probe the local carrier concentration in a device. In our sample the separation of charge at 6 T and 50 μA was $0.036N_s$; this was superimposed on a 2% inhomogeneity in N_s.

ACKNOWLEDGMENTS

The authors would like to thank S. Chapman for help in setting up the imaging system. We are grateful to K. von Klitzing and V. Fal'ko for stimulating criticism. One of us (A.S.) thanks L. J. Challis who kindly organized his visit to the University of Nottingham. This work was supported by a grant from the SERC of the U.K.

*Permanent address: A. F. Ioffe Physical Technical Institute, 26 Polytechnicheskaya, 194021 St. Petersburg, Russia.

[1]B. I. Halperin, Phys. Rev. B **25**, 2185 (1982).
[2]A. H. MacDonald and P. Streda, Phys. Rev. B **29**, 1616 (1984).
[3]M. Büttiker, Phys. Rev. B **38**, 9375 (1988).
[4]S. Komiyama and H. Hirai, Phys. Rev. B **40**, 7767 (1989).
[5]P. C. van Son, G. H. Kruithof, and T. M. Klapwijk, Phys. Rev. B **42**, 11 267 (1990).
[6]S. Komiyama, H. Hirai, S. Sasa, and S. Hiyamizu, Phys. Rev. B **40**, 12 566 (1989).
[7]B. J. van Wees, E. M. M. Willems, C. J. P. M. Haarmans, C. W. J. Beenakker, H. van Houten, J. G. Williamson, C. T. Foxon, and J. J. Harris, Phys. Rev. Lett. **62**, 1181 (1989).
[8]R. Merz, F. Keilmann, R. J. Haug, and K. Ploog, Phys. Rev. Lett. **70**, 651 (1993).
[9]S. Komiyama, H. Hirai, M. Ohsawa, Y. Matsuda, S. Sasa, and T. Fujii, Phys. Rev. B **45**, 11 085 (1992).
[10]P. L. McEuen, A. Szafer, C. A. Richer, B. W. Alphenaar, J.

K. Jain, A. D. Stone, R. G. Wheeler, and R. N. Sacks, Phys. Rev. Lett. **64**, 2062 (1990).
[11]R. J. Haug and K. von Klitzing, Europhys. Lett. **10**, 489 (1989).
[12]A. J. Kent, V. W. Rampton, M. I. Newton, P. J. A. Carter, G. A. Hardy, P. Hawker, P. A. Russell, and L. J. Challis, Surf. Sci. **196**, 410 (1988).
[13]A. J. Kent, G. A. Hardy, P. Hawker, V. W. Rampton, M. I. Newton, P. A. Russell, and L. J. Challis, Phys. Rev. Lett. **61**, 180 (1988).
[14]A. J. Kent, D. J. McKitterick, L. J. Challis, P. Hawker, C. J. Mellor, and M. Henini, Phys. Rev. Lett. **69**, 1684 (1992).
[15]W. A. Little, Can. J. Phys. **37**, 334 (1959).
[16]B. Taylor, H. J. Maris, and C. Elbaum, Phys. Rev. Lett. **23**, 416 (1969).
[17]A. J. Kent, Physica **B169**, 356 (1991).
[18]H. J. Fischbeck and J. Mertsching, Phys. Status Solidi **31**, 107 (1969).
[19]V. F. Gantmakher and I. B. Levinson, *Carrier Scattering in Metals and Semiconductors* (North-Holland, Amsterdam, 1987).
[20]J. P. Leburton, S. Briggs, and D. Jovanovich, Superlatt. Microstruct. **8**, 209 (1990).
[21]J. P. Leburton and D. Jovanovich, Semicond. Sci. Technol. **7**, B202 (1992).
[22]S. M. Badalian, Y. B. Levinson, and D. L. Maslov, Pis'ma Zh. Eksp. Teor. Fiz. **53**, 595 (1991) [JETP Lett. **53**, 619 (1991)].
[23]H. J. Fischbeck and J. Mertsching, Phys. Status Solidi **31**, K157 (1969).
[24]A. Y. Shik, Fiz. Tekh. Poluprovodn. **26**, 855 (1992) [Sov. Phys. Semicond. **26**, 481 (1992)].
[25]E. A. Kaner, N. M. Makarov, and I. M. Fuks, Zh. Eksp. Teor. Fiz. **55**, 931 (1968) [Sov. Phys. JETP **28**, 483 (1968)].
[26]T. Martin and S. Feng, Phys. Rev. Lett. **64**, 1971 (1990).
[27]R. J. Nicholas, R. J. Haug, K. von Klitzing, and G. Weimann, Phys. Rev. B **37**, 1294 (1988).

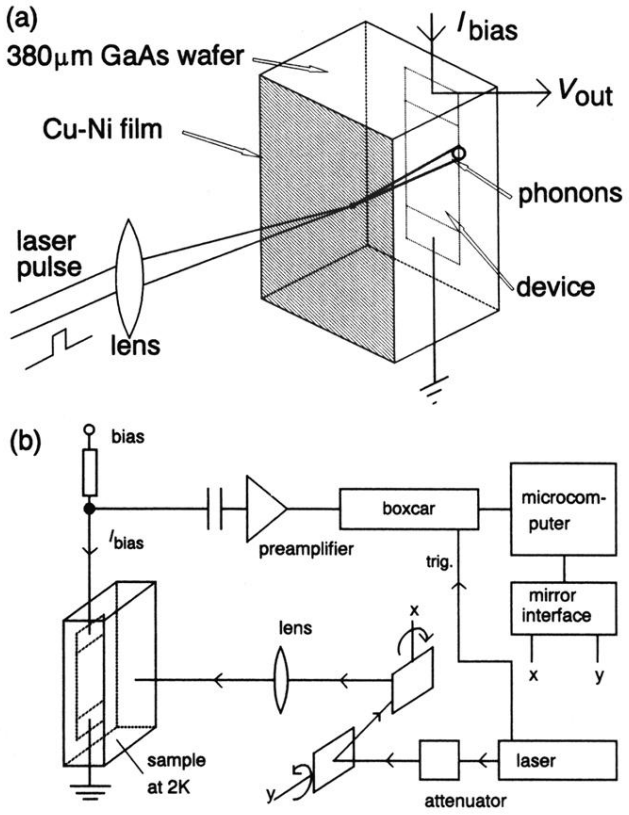

FIG. 2. (a) Sample geometry: nonequilibrium phonons are generated by thermalizing a pulsed laser in a Cu-Ni film. These propagate across the GaAs substrate ballistically and interact with the 2DEG giving rise to a transient change in V_{out} at constant bias current. (b) Schematic diagram of the full imaging system: The laser beam is positioned using a pair of galvanometer-driven mirrors and the signal is recorded as a function of the beam position.

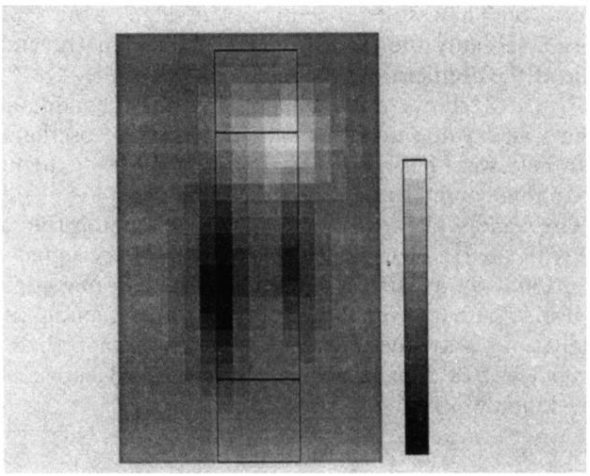

FIG. 4. 2D image of the sample response at integer filling factor (magnetic field 1.5 T, directed into paper; current 50 μA, up). The dark regions at the edges of the sample are due to a decrease in conductance when the phonons are incident there. Note also the activated behavior (bright region) when the phonons are incident at the point where current exits (electrons enter) the 2DEG.

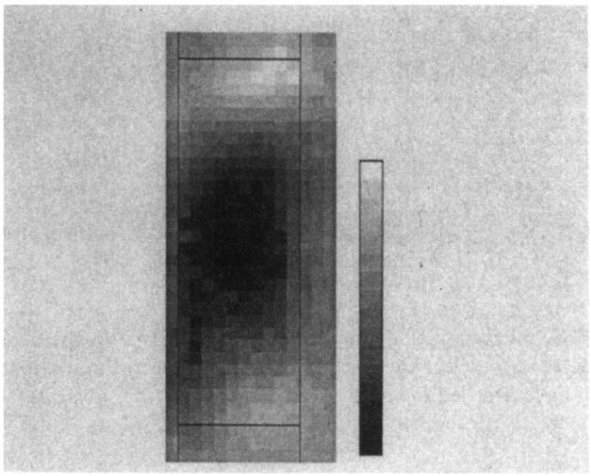

FIG. 6. Image of the phonoconductivity response on one of the spin-split peaks (field and current directions as in Fig. 4).

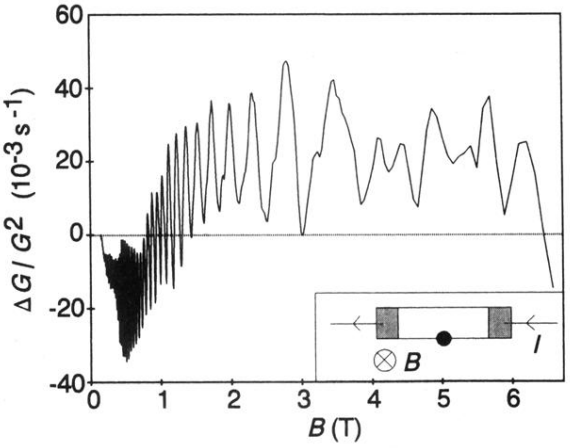

FIG. 7. Variation with magnetic field of the phonoconductivity at the opposite edge to that in Fig. 5.

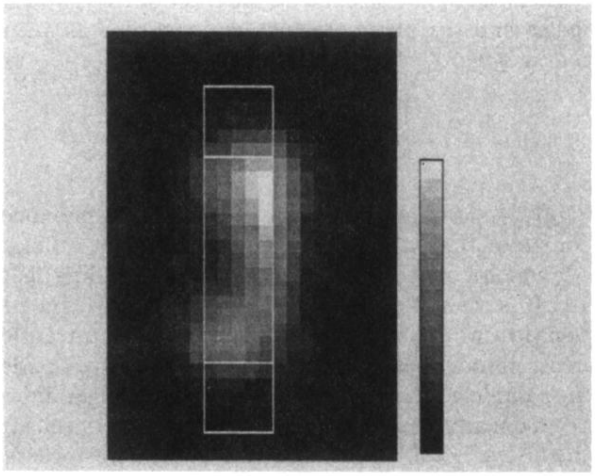

FIG. 8. Image of the positive phonoconductivity showing that this too is an edge effect.